

Thermal conduction in accretion disk coronae

Andrzej Maciołek–Niedźwiecki¹, Julian H. Krolik² and Andrzej A. Zdziarski¹

ABSTRACT

We study the effects of thermal conduction in a hot, active corona above an accretion disk. We assume that all of the dissipative heating takes place in the corona. We find that the importance of conduction decreases with increases in the local dissipative compactness of the corona, $\ell_{\text{diss,loc}}$, and increases with increasing abundance of electron-positron pairs. For $\ell_{\text{diss,loc}} < 1$, a significant fraction of the energy released in the corona may be carried away by the conductive flux, leading to formation of a relatively hot transition layer below the base of the corona. Comptonization of disk radiation in such a layer may account for the presence of soft X-ray excesses in the spectra emitted by disk-corona systems.

Subject headings: accretion, accretion disks — conduction — galaxies: active — X-rays: galaxies

1. INTRODUCTION

An accretion disk with a dissipative, thermal corona has recently become a popular model for interpreting the UV/X/ γ -ray spectra from Seyfert galaxies and Galactic black hole candidates (see, e.g., Svensson 1996). Recent studies have focused on the correct description of the spectrum from such a system (e.g., Stern et al. 1995, Poutanen & Svensson 1996, Sincell & Krolik 1997) whereas relatively little effort has been taken to achieve a physically self-consistent internal structure of the corona. In particular, most of the existing models of disk-corona systems involve two simplifying assumptions: isothermal structure of the corona, and purely radiative energy exchange between the corona and the disk. We relax the above assumptions by considering effects of thermal conduction, which will obviously occur in a hot corona situated above the surface of a cold disk. Such a treatment allows us to determine self-consistently the electron density and temperature distributions in the corona.

We consider two limiting cases: a corona consisting purely of electron-positron pairs, and a corona without pairs (a pure electron-proton plasma). The calculations of thermal pair equilibria (e.g., Stern et al. 1995) show that both cases (e^\pm and ep dominated coronae) may be expected in accreting black hole systems, depending on both the compactness (defined below) and the temperature. We assume that ep coronae satisfy the condition of hydrostatic equilibrium. For e^\pm coronae, the hydrostatic model is inconsistent and large-scale coronal expansion is expected, as we discuss in section 2.5. Leaving the investigation of the exact structure of pair coronae for future studies, we consider here a constant pressure structure to see what effect conduction may have in the presence of pairs.

2. PHYSICAL PROCESSES IN A CORONA

¹N. Copernicus Astronomical Center, Bartycka 18, 00-716 Warsaw, Poland

²Department of Physics and Astronomy, Johns Hopkins University, Baltimore, MD 21218, USA

2.1. Notation and basic assumptions

We assume that the corona has a slab geometry with a scale height h and a surface area A . We also assume a sandwich geometry (coronae located on both sides of the disk) so that we can consider only half of such a plane symmetrical system. The plasma in the corona is assumed to be optically thin ($\tau_{\text{tot}} \lesssim 1$, where $\tau_{\text{tot}} = \sigma_T \int_0^h n_e(z) dz$ is the total optical depth, n_e is the electron density, and z is the distance from the corona bottom) and to have a thermal distribution of electron energies (with the temperature varying across the corona). These assumptions are supported by observations of Seyfert 1 galaxies (e.g., Zdziarski et al. 1995; Gondek et al. 1996) and Galactic black hole candidates (e.g., Gierliński et al. 1997), whose spectra are well fitted by optically thin thermal Comptonization.

We measure the electron density and the temperature of the plasma by the following dimensionless parameters,

$$\Theta \equiv \frac{kT}{m_e c^2}, \quad (1)$$

$$\tau_x \equiv n_e(x) \sigma_T h, \quad (2)$$

where $x \equiv z/h$. The latter parameter is the differential Thomson depth at x in the interval dx , i.e. $\tau_x = d\tau/dx$, where $d\tau = n_e(z) \sigma_T dz$.

Following Haardt & Maraschi (1991, 1993), we assume that most of the accretion energy is dissipated in the corona. The dissipated power is lost due to thermal conduction and radiation losses. Half of the high energy radiation from the corona irradiates the cold disk and the other half escapes directly from the source (we neglect for simplicity the anisotropy of the scattering process in the corona and reflection of hard photons from the cold matter). The coronal radiation intercepted by the disk is reprocessed and reemitted at much lower energies, which provides soft seed photons for Comptonization in the corona. The dissipated power, L_{diss} , and both the corona and disk radiation luminosities, L_h and L_s , respectively, are characterized by compactness parameters:

$$\ell_{\text{diss}} \equiv \frac{L_{\text{diss}}}{h} \frac{\sigma_T}{m_e c^3}, \quad \ell_h \equiv \frac{L_h}{h} \frac{\sigma_T}{m_e c^3}, \quad \ell_s \equiv \frac{L_s}{h} \frac{\sigma_T}{m_e c^3}. \quad (3)$$

[L_h and L_s correspond to the total power of radiation emitted by one side of the corona and the disk, while the observed luminosities of those layers are described by $L_h/2$ and $\sim L_s \exp(-\tau_{\text{tot}})$, respectively.] Our main parameter is, however, the local dissipative compactness parameter (introduced by Björnsson & Svensson 1992),

$$\ell_{\text{diss,loc}} \equiv \frac{L_{\text{diss,loc}}}{h} \frac{\sigma_T}{m_e c^3}, \quad (4)$$

where $L_{\text{diss,loc}} = L_{\text{diss}} h^3 / (Ah)$, and thus

$$\ell_{\text{diss,loc}} = \ell_{\text{diss}} \frac{h^2}{A}. \quad (5)$$

This parameter is crucial for determining the efficiency of radiative processes in the corona, since it involves the luminosity in a cubic volume with the size h , which is the characteristic local volume in the corona. Analogously, we define the local radiative compactnesses,

$$\ell_{h,\text{loc}} = \ell_h \frac{h^2}{A}, \quad \ell_{s,\text{loc}} = \ell_s \frac{h^2}{A}. \quad (6)$$

We emphasize the importance of the difference between the local compactness and global compactness, $\ell_{\text{glob}} \equiv L \sigma_T / (R m_e c^3)$, where R is the distance from the central source, in the corona geometry (see also

Gondek et al. 1996). It is the local compactness which is the most relevant for parameterizing the character of the coronal thermal and pair balance, which fact is clear from the form of our equations (38–40) below. It is equally true for other problems, for example, for the issue of whether the electrons in the corona can achieve a thermal distribution function (cf. Ghisellini et al. 1993). The electron distribution function is determined by a competition between the electron-electron relaxation timescale (determined by the electron density and mean energy) and the electron cooling timescale (which depends on the radiation energy density). Their ratio is then a function of the optical depth and the *local* compactness, not the *global* compactness. Since ℓ_{loc} is always smaller than ℓ_{glob} , and sometimes very much smaller, this can be an important distinction. The cooling time becomes relatively longer as ℓ falls, so using ℓ_{glob} instead of ℓ_{loc} can lead to a spurious difficulty in achieving an equilibrium distribution function.

The importance of the conduction process will be measured by the fraction of the dissipated power transported out of the corona by the conductive flux,

$$\epsilon_q = \frac{|q_0|A}{L_{\text{diss}}}, \quad (7)$$

where q_0 is the heat flux through the corona bottom.

Taking into account both the radiative energy exchange and the conductive transport of thermal energy, we can relate the corona and disk luminosities to the dissipated power,

$$L_{\text{h}} = L_{\text{diss}}(1 - \epsilon_q), \quad L_{\text{s}} = 0.5L_{\text{h}} + \epsilon_q L_{\text{diss}}, \quad (8)$$

(we neglected here the initial energy of soft photons scattered in the corona as they contribute negligibly to the corona luminosity). Then

$$\frac{\ell_{\text{s}}}{\ell_{\text{diss}}} = 0.5(1 + \epsilon_q), \quad \frac{\ell_{\text{h}}}{\ell_{\text{diss}}} = 1 - \epsilon_q. \quad (9)$$

2.2. Heating

We assume that all electrons in the corona are heated at a constant rate, γ . Then the heating rate per unit volume is,

$$H = \gamma n_e(z), \quad (10)$$

which corresponds to a local dissipative compactness,

$$\ell_{\text{diss,loc}} = \Gamma \tau_{\text{tot}}, \quad (11)$$

where

$$\Gamma = \frac{\gamma}{m_e c^2} \frac{h}{c}. \quad (12)$$

2.3. Radiative processes

Radiative cooling in the corona is due to unsaturated Comptonization and bremsstrahlung. The Compton cooling rate is

$$C_{\text{Compt}} = \max(4\Theta, 16\Theta^2) n_e c \sigma_{\text{T}} U_{\text{rad}}, \quad (13)$$

where U_{rad} is the radiation energy density, n_e is the electron density, and the expressions in parentheses give the average relative photon energy gain per scattering in the nonrelativistic (4Θ) and relativistic ($16\Theta^2$) cases, respectively (for $0.2 < \Theta < 0.3$, we use $80\Theta^3 - 32\Theta^2 + 7.2\Theta$ in order to achieve a smooth transition between the two regimes). We take into account cooling of electrons on both soft photons from the disk and photons already scattered in the corona. As photons scattered many times in the corona may enter the Klein-Nishina regime, we include only photons satisfying the condition

$$\varepsilon < \min(\Theta^{-1}, 1) \quad (14)$$

where $\varepsilon \equiv h\nu/m_e c^2$. Then,

$$U_{\text{rad}} = \frac{1}{c} \frac{L_s + \eta L_h}{A}, \quad (15)$$

where the fraction of the energy density that scatters in the Thomson regime is

$$\eta = \frac{\int_{\varepsilon_0}^{\min(1/\Theta, 1)} F(\varepsilon) d\varepsilon}{\int_{\varepsilon_0}^{\infty} F(\varepsilon) d\varepsilon}, \quad (16)$$

$F(\varepsilon)$ is the energy spectrum of the hard radiation from the corona [we assume a power-law spectrum with the energy index given by eqs. (1) and (2) in Zdziarski et al. (1994) and an exponential cut-off at $E_c = 1.6kT$], and ε_0 is the soft photons' energy. The bremsstrahlung cooling rate is

$$C_{\text{brem}} = n_e^2 m_e c^3 \sigma_T l_{\text{brem}}(\Theta), \quad (17)$$

where

$$l_{\text{brem}}(\Theta) = \begin{cases} 4\sqrt{2}\alpha_f \pi^{-3/2} (\Theta^{1/2} + 1.781\Theta^{1.84}), & \Theta \leq 1, \\ 4.5\alpha_f \pi^{-1} [\ln(1.12\Theta + 0.42) + 1.5], & \Theta \geq 1, \end{cases} \quad (18)$$

and α_f is the fine-structure constant (Svensson 1982).

2.4. Thermal conduction

The classical heat flux is expressed by

$$q_{\text{class}} = -\kappa \frac{dT}{dz}, \quad (19)$$

where κ is the thermal conductivity. In a fully ionized hydrogen plasma,

$$\kappa = \phi_c \chi T^{\frac{5}{2}}, \quad (20)$$

where the parameter ϕ_c allows for a reduction of the heat flux by magnetic fields, turbulence etc. (and is taken here to be $\phi_c = 1$) and

$$\chi = 18 \left(\frac{2}{\pi} \right)^{3/2} \frac{k^{7/2}}{m_e^{1/2} e^4 \ln \Lambda} \quad (21)$$

(Spitzer 1962), where

$$\ln \Lambda = 29.7 + \ln [(T_e/10^6 \text{K}) n_e^{-1}] \quad (22)$$

is the Coulomb logarithm. As $\ln \Lambda$ depends logarithmically on electron density and temperature, we assume a constant value of $\ln \Lambda = 30.7$, which corresponds to $\chi = 6 \times 10^{-7} \text{erg s}^{-1} \text{cm}^{-1} \text{K}^{-7/2}$. The classical

expression for the heat flux is based on the assumption that the electron mean free path is short compared to the temperature height scale, $T/|\nabla T|$. In the limit $|\nabla T| \rightarrow \infty$ the heat flux is said to be “saturated”, and Cowie & McKee (1977) suggested the form

$$|q_{\text{sat}}| = 5\phi_s \rho c_s^3, \quad (23)$$

where $c_s = (kT/\mu)^{1/2}$ is the isothermal sound speed, μ is the mean mass per particle ($\mu \approx m_p/2$ for ep plasmas and m_e for e^\pm plasmas), ρ is the mass density and ϕ_s parametrizes the uncertainty of the appropriate value of q_{sat} . Both experimental and theoretical results constrain ϕ_s to the range $\phi_s = 0.2$ – 1.1 with some preference for the value of $\phi_s = 0.3$ (Balbus & McKee 1982; Giuliani 1984). We use here $\phi_s = 0.3$ but test the sensitivity of the results to the value of ϕ_s . The saturated heat flux given by eq. (23) corresponds to advection of the plasma’s thermal energy at a rate comparable to the sound speed. In order to smoothly implement the transition from classical diffusive to saturated transport, Balbus & McKee (1982) defined the effective heat flux as the harmonic mean of q_{sat} and q_{class} ,

$$q = -\frac{\kappa}{1 + \sigma} \frac{dT}{dz}, \quad (24)$$

where

$$\sigma = \left| \frac{q_{\text{class}}}{q_{\text{sat}}} \right|. \quad (25)$$

The equation of heat transfer in the vertical direction,

$$\frac{dq}{dz} = H - C_{\text{Compt}} - C_{\text{brem}}, \quad (26)$$

may then be written in a dimensionless form,

$$\frac{d}{dx} \left(\frac{a\Theta^{5/2}}{1 + b\Theta|\Theta'|} \Theta' \right) = f(\Theta, \tau_x), \quad (27)$$

where

$$f(\Theta, \tau_x) = \ell_{\text{diss,loc}} \tau_x \frac{\ell_s + \eta \ell_h}{\ell_{\text{diss}}} \max(4\Theta, 16\Theta^2) - \Gamma \tau_x + l_{\text{brem}}(\Theta) \tau_x^2, \quad (28)$$

$$a \equiv \phi_c \chi \left(\frac{m_e c^2}{k} \right)^{7/2} \frac{\sigma_T}{m_e c^3}, \quad (29)$$

$$b \equiv \frac{1}{\tau_x} \frac{a}{5\phi_s \delta} \left(\frac{\mu}{m_e} \right)^{1/2}, \quad (30)$$

$$\Theta' \equiv \frac{d\Theta}{dx}, \quad (31)$$

and $\delta = 1$ and 2 for electron-positron and electron-proton plasmas, respectively.

2.5. Hydrostatic equilibrium

For an electron-proton corona, the condition $h \ll R$ is satisfied and the following approximate form of the hydrostatic equilibrium equation may be used,

$$\frac{dP}{dz} = -\frac{GM}{R^3} (z + z_d) \rho(z), \quad (32)$$

where P is the pressure in the corona and z_d is the distance of the corona bottom from the disk midplane. The pressure is the sum of radiation and gas pressures. From

$$\frac{P_{\text{rad}}}{P_{\text{gas}}} = \ell_{\text{diss,loc}} \frac{\ell_s + \ell_h}{\ell_{\text{diss}}} \frac{1}{2\Theta\tau}, \quad (33)$$

$\Theta\tau \approx 0.1(\ell_h/\ell_s)^{1/4}$ (Pietrini & Krolik 1995), and eq. (9) (with $\epsilon_q < 0.5$, as found in section 4), we find that the gas pressure dominates for $\ell_{\text{diss,loc}} < 0.15$. At higher compactnesses thermal conduction becomes unimportant (section 4), so we neglect radiation pressure. Then equation (32) with $P = 2n_e kT$ gives

$$\frac{d\tau_x}{dx} = -\frac{\tau_x}{\Theta} \left[\Theta' + \frac{1}{4r} \frac{m_p}{m_e} \left(\frac{h}{R} \right)^2 (x + x_d) \right], \quad (34)$$

where $x_d = z_d/h$, $r = R/R_{\text{Sch}}$ and $R_{\text{Sch}} \equiv 2GM/c^2$. For an isothermal corona the above equation gives,

$$(h/R)^2 = 8r \frac{m_e}{m_p} \Theta_c, \quad (35)$$

where Θ_c is the (constant) temperature of the corona. In section 4 we find that thermal conduction significantly affects the corona structure near its base in a way that may increase the corona total optical depth. However, the temperature at higher altitudes is roughly constant and the density profile does not differ from that found in isothermal approximation. Therefore, we use the scale height determined by eq. (35), approximating Θ_c by the temperature at the top of the corona, Θ_{top} (see section 2.7).

The distance, z_d , is the sum of the disk height, h_{disk} , and the height of the transition layer affected by thermal conduction, h_{tl} . Using the results of Svensson & Zdziarski (1994), we find that the ratio of corona height to disk height is $h/h_{\text{disk}} \gtrsim 100$. The value of h_{tl} is determined by the solution of the conduction problem and (as we find in section 4) typically $h_{\text{tl}} \gtrsim 0.1h$ when conduction is important. In this case, the value of z_d is dominated by the height of the transition layer. The exact value can be obtained with additional parameters of the model (accretion rate, viscosity parameter etc.) necessary for the calculation of h_{disk} .

For electron-positron coronae, the gravitational force acting on the corona is too small to keep it bound because the escape speed is $\sim cr^{-1/2}$, whereas the sound speed is $\sim c \min(1/\sqrt{3}, \Theta^{1/2})$ and Compton equilibrium generically gives temperatures Θ not much less than unity. Consequently, in a pure pair plasma $h \sim R$ and strong outflows can be expected unless the plasma is confined by magnetic fields.

In order to check the importance of thermal conduction in pair coronae, we consider here a zone of e^\pm plasma at low altitudes above the disk (as it is unlikely that the heating mechanism operates at large distances from the disk) close to hydrostatic equilibrium so that the corona exists. As the pressure gradient induced by the pair gravity is negligible, we expect that such a zone is almost isobaric and so we will describe that zone by eq. (34) with the null gravity term (the second term in brackets).

2.6. Transition layer

As we find in section 4 below, the bottom of the corona is much hotter than the disk. Thus a transition layer between the disk and the corona must exist over which the temperature decreases from the coronal to disk value. Decrease of the temperature in the transition layer is accompanied by a decrease of conductive heat flux, as the energy transported from the disk is gradually radiated away. At some point the conductive

flux vanishes and the temperature levels off at a value determined by the balance between radiative heating and cooling. We call this point the base of the transition layer. Below the base the temperature is still higher than the “normal” disk temperature, due to Compton heating by the coronal radiation. We do not investigate properties of that Compton heated layer as atomic processes (which are neglected in this paper) may become important there (a detailed analysis of such regions has recently been done by Róžańska & Czerny 1996 and Sincell & Krolik 1997).

The structure of the transition layer affected by thermal conduction may be found in the framework of our model with $H = 0$. We take into account Compton heating of electrons in the transition layer. Then the right-hand side of the heat transfer equation (27) takes the form,

$$\begin{aligned} f(\Theta, \tau_x) = & \ell_{\text{diss,loc}} \tau_x \left\{ 0.5 \eta \exp\left(-\int_x^0 \tau_x dx\right) \ell_h \ell_{\text{diss}}^{-1} [\max(4\Theta, 16\Theta^2) - \langle \varepsilon \rangle] \right. \\ & \left. + \ell_s \ell_{\text{diss}}^{-1} [\max(4\Theta, 16\Theta^2) - \langle \varepsilon_0 \rangle] \right\} + l_{\text{brem}}(\Theta) \tau_x^2, \end{aligned} \quad (36)$$

where η is given by eq. (16) and

$$\langle \varepsilon \rangle = \frac{\int F \varepsilon d\varepsilon}{\int F d\varepsilon}. \quad (37)$$

The integrals over the energy spectrum of the radiation emitted from the corona have upper limits equal of $\min(\Theta^{-1}, 1)$, and $\langle \varepsilon_0 \rangle = 5 \times 10^{-5}$ is assumed for soft radiation from the disk. (For Galactic black hole candidates, $\langle \varepsilon_0 \rangle = 10^{-3}$ would be a more appropriate value, but the results depend weakly on this parameter.)

While for ep coronae the transition layer will obviously consist of an electron-proton plasma, the composition of the transition layer for e^\pm coronae is rather uncertain and depends on the mechanism of formation of the transition layer. If it is formed by the heating of the outer parts of the accretion disk, we can expect that it is composed mostly of ep with some addition of pairs inflowing from the corona. On the other hand, the transition layer may be formed together with the active region and then it would be dominated by electron-positron plasma. We will examine here the latter possibility (by assuming that both the corona and the transition layer consist only of e^\pm plasma) to estimate the maximum effect of thermal conduction, which is achieved for a pure pair plasma (see section 4).

3. CALCULATIONAL PROCEDURE

3.1. Differential Equations

Eqs. (27) and (34) give three first-order differential equations,

$$\frac{d\Theta}{dx} = \Theta', \quad (38)$$

$$\frac{d\Theta'}{dx} = f(\Theta, \tau_x) \frac{(1 + b\Theta\Theta')^2}{a\Theta^{2.5}} + b\Theta'^2 g(x + x_d) - 0.5b\Theta'^3 - 2.5 \frac{\Theta'^2}{\Theta}, \quad (39)$$

$$\frac{d\tau_x}{dx} = -\frac{\tau_x}{\Theta} [\Theta' + g(x + x_d)], \quad (40)$$

where $f(\Theta, \tau_x)$ is given by eqs. (28) and (36) for the corona and the transition layer, respectively, and

$$g = \begin{cases} 2\Theta_c, & \text{for proton-electron plasma,} \\ 0, & \text{for electron-positron plasma.} \end{cases} \quad (41)$$

The null value of g for e^\pm coronae results from the isobaric approximation, whereas $g \equiv (h/R)^2 m_p / (4rm_e)$ for ep coronae. We solve the above equations for $\Theta(x)$, $\Theta'(x)$ and τ_x .

3.2. Parameters and Boundary Conditions

We are solving three first-order differential equations which depend on two dimensionless parameters, τ_{tot} and $\ell_{\text{diss,loc}}$. Thus, in addition to choosing the parameters, we must also choose three boundary conditions, Θ_{top} , Θ'_{top} , and τ_x at the top of the corona, which we call τ_{top} .

The physically appropriate choice for the temperature gradient is obvious. There should be no heat flux at the top of the corona, so

$$\left. \frac{d\Theta}{dx} \right|_{\text{top}} = 0. \quad (42)$$

The other boundary conditions are subtler to determine. In the absence of conduction, the temperature throughout the corona would be determined by $\ell_{\text{diss,loc}}$ and τ_{tot} . This is the calculation performed in numerous other discussions of accretion disk coronae. However, heat conduction removes some heat from the corona, decreasing its temperature, and we do not know how much this affects the top of the corona before doing the calculation. We implicitly fix Θ_{top} by setting the temperature at the bottom of the transition layer to be effectively zero, or at least far below the coronal temperature. The value used to initiate the integration is then a parameter to be iterated on until self-consistency (see the Appendix for details).

The third boundary condition, τ_{top} , may be thought of as the density at the top of the corona. Because we have normalized our unit of distance to the scale height, it is implicitly fixed by τ_{tot} . In the case of an ep plasma, the density profile of the corona is approximately Gaussian (it would be exactly Gaussian if the temperature were exactly independent of height), so formally the corona extends to infinity. However, we must choose some finite number of scale lengths at which to bound our calculation. We do so by setting the differential Thomson depth at the top $\tau_{\text{top}} = 0.0001$. If the corona were exactly isothermal, this would be achieved at $x_{\text{top}} = \ln^{1/2}(\tau_{\text{tot}}/\tau_{\text{top}})$, so by starting the integration at x_{top} with $\tau_{\text{top}} = 0.0001$, all would be self-consistent. To account for the deviations from isothermality induced by conduction, we iterate on x_{top} , keeping τ_{top} fixed at 0.0001. In the case of a pair plasma, our constant pressure assumption translates to a density profile which approaches closer and closer to a step-function in the limit as the temperature profile approaches isothermal. We therefore start the calculation at $x = 1$ and assume an initial value of the coronal pressure. Then we adjust the value of the pressure to obtain the assumed τ_{tot} .

The optical depth, τ_{tot} , and the local compactness, $\ell_{\text{diss,loc}}$, of the corona are the main parameters of the model. x_d is also a free parameter, but its value can be determined for a specific disk model, as discussed in section 2.5. Increase of x_d results in a slight increase of ϵ_q , due to the change of the density profile in the corona. The solution of the transition layer structure gives an obvious constraint on the value of x_d , which must exceed the height of the transition layer. We assume an initial value of ϵ_q , which determines $\ell_s/\ell_{\text{diss}}$ and $\ell_h/\ell_{\text{diss}}$ from eq. (9). The value of Γ follows from eq. (11).

Summarizing, our model has three free parameters, τ_{tot} , $\ell_{\text{diss,loc}}$ and x_d . In calculations, we first adjust Θ_{top} and x_{top} (or P_{gas} for e^\pm coronae) as described above. Then the value of ϵ_q from the solution with adjusted Θ_{top} and x_{top} is used in the next iteration. The procedure ends when the calculated value of ϵ_q converges. As discussed in Appendix A, once the three free parameters are specified, there is a (narrow)

allowed range ($\Theta_{\text{top}}, \Theta_{\text{top}} + \Delta\Theta$) (and a corresponding range of x_{top}) within which acceptable solutions exist. The members of this solution family are distinguished by the pressure at the bottom of the transition zone.

For *ep* coronae we computed solutions for $0.01 \leq \ell_{\text{diss,loc}} \leq 0.4$, while in the pair case we found solutions for $0.01 \leq \ell_{\text{diss,loc}} \leq 10$. The lower limit on $\ell_{\text{diss,loc}}$ was suggested by both the observational results [see, e.g., table 1 in Done & Fabian (1989) noting that the local compactness is roughly an order of magnitude lower than the global compactness given there] and theoretical expectations [for slab coronae $\ell_{\text{diss,loc}} < 0.01$ corresponds to $L < 10^{-3} L_{\text{Edd}}$ (see section 5) which is unlikely in AGNs]. Note that for $\ell_{\text{diss,loc}} < 0.1$ the corona may still be pair dominated (see, e.g., figure 1 in Stern et al. 1995). The upper limits are set by the character of our solutions: at higher $\ell_{\text{diss,loc}}$ conduction becomes negligible (see below). For both e^\pm and *ep* coronae, the optical depth range over which we computed solutions was $0.06 < \tau_{\text{tot}} < 0.3$.

4. RESULTS

We find that heat flux saturation puts an important constraint on the conduction problem in that it establishes a limit on the amount of thermal energy that can be transported out of the corona. Namely, the conductive heat flux at the bottom cannot exceed the saturated heat flux,

$$q_{\text{sat}} = 5\phi_s \delta \left(\frac{m_e}{\mu} \right)^{1/2} \frac{m_e c^3}{\sigma_T h} \tau \Theta^{3/2}. \quad (43)$$

As this limit is independent of the total amount of released power, the relative importance of the thermal conduction process increases with decreasing compactness. The maximum fraction of the released power that can leave the corona in the form of conductive flux is,

$$\frac{q_{\text{sat}} A}{L_{\text{diss}}} = \frac{5\phi_s \delta (m_e/\mu)^{1/2} \tau \Theta^{3/2}}{\ell_{\text{diss,loc}}}. \quad (44)$$

As discussed below, the temperature cannot differ strongly from the Compton equilibrium value, which can be estimated from $\Theta\tau \simeq 0.1(l_h/l_s)^{1/4}$ (Pietrini and Krolik 1995). Then $l_h/l_s \leq 2$ [eq. (9)] implies,

$$\frac{q_{\text{sat}} A}{L_{\text{diss}}} \leq 0.2 \frac{\delta (m_e/\mu)^{1/2} \Theta^{1/2}}{\ell_{\text{diss,loc}}}, \quad (45)$$

where we assumed $\phi_s = 0.3$. As $\Theta \lesssim 1$ in both Seyfert galaxies and black hole binaries (e.g., Zdziarski et al. 1997), we find that conduction has a rather minor effect (transporting less than 5 per cent of the released power) for $\ell_{\text{diss,loc}} \gtrsim 1$ and $\ell_{\text{diss,loc}} \gtrsim 0.15$ for electron-positron and electron-proton plasmas, respectively.

Figures 1 and 2 show the dependence of ϵ_q on $\ell_{\text{diss,loc}}$. The relation suggested by eq. (45), $\epsilon_q \propto \ell_{\text{diss,loc}}^{-1}$, appears to be valid for $\ell_{\text{diss,loc}} \gtrsim 1$ and $\ell_{\text{diss,loc}} > 0.04$ for e^\pm and *ep* plasmas, respectively. For lower values of $\ell_{\text{diss,loc}}$, the dependence rolls over to approach the classical heat flux case in the limit of very small compactness (in numerical calculations we obtain the classical heat flux limit by setting $\phi_s = 1000$). Figure 3 shows the dependence of ϵ_q on τ_{tot} . For lower local compactness parameters, ϵ_q decreases with increasing τ_{tot} due to a higher radiative cooling efficiency of the corona. For higher $\ell_{\text{diss,loc}}$ (in the saturation regime), ϵ_q is only weakly dependent on τ_{tot} ; an increase of the cooling efficiency with τ_{tot} is compensated by an increase of the saturated heat flux (due to the increase of τ_x).

Solid curves on Figures 4 and 5 show the temperature, the dimensionless electron density and the heat flux profiles in the corona ($x > 0$) and in the transition layer ($x < 0$) obtained within our thermal

conduction model. The dashed curves show the solutions of the model in which conduction is neglected (the temperature here is determined by the equilibrium between heating and cooling).

Saturation prevents the temperature in the corona from being much lower than the Compton equilibrium temperature. Namely, a decrease of the temperature results in a decrease of the radiative cooling efficiency, which increases the amount of energy that must be taken out of the corona by the conductive flux. This quickly exceeds the capability of the saturated transport. The amount by which the corona temperature may deviate from the Compton equilibrium value depends on the local compactness. At values of $\ell_{\text{diss,loc}}$ for which conduction is important, the difference may become significant (Figures 4 and 5, left panels). In this case, conduction leads to an observationally interesting effect of the softening of the spectrum, as a lower plasma temperature is achieved while the optical depth remains unchanged. For higher compactness parameters, only a tiny difference is possible and then most of the coronal emission comes from a roughly isothermal region (Figures 4 and 5, right panels).

The transition layer formed below the base of the corona has a relatively high temperature and may extend over a height of a few tenths of the corona height scale, as shown by solid curves at $x < 0$ on Figures 4 and 5. The existence of such a layer was overlooked in previous studies of the disk-corona interface (e.g., Shimura et al. 1995) as they neglected conduction, which appears to provide the major contribution of energy to that region. Indeed, by comparing the energy input to the transition layer due to the maximum (saturated) value of conductive flux with the energy input due to heat flux of coronal radiation, we find that

$$\frac{q_{\text{sat}}}{H_{\text{Compt}} h_{\text{tl}}} = \frac{5\phi_s \delta \tau \Theta^{3/2}}{\ell_{\text{h,loc}} \langle \varepsilon \rangle \tau_{\text{tl}} \eta} \left(\frac{m_e}{\mu} \right)^{1/2}, \quad (46)$$

where τ_{tl} is the optical depth of the transition layer and $\langle \varepsilon \rangle$ is given by eq. (37). From this we find that, e.g., for the parameters of the model shown on the right panel of Figure 4 conduction provides 10 times more energy than Compton heating. The weak contribution of Compton heating is due to the fact that the average energy of photons emitted by unsaturated Comptonization is much lower than the average electron energy in that plasma. Then, if a purely radiative energy exchange between two phases of a plasma occurs, the irradiated phase achieves a much lower temperature than the hot one. For a disk-corona system this would lead to a sharp decline in the temperature profile, as shown by dashed curves on Figures 4 and 5. The optical depth and Compton parameter, $y_{\text{tl}} = \int_{x_{\text{tl}}}^0 (4\Theta + 16\Theta^2) \tau_x dx$, of the transition layer decrease with increasing local compactness (because a lower y_{tl} is needed at higher luminosity for the loss of the transported energy), e.g. $\tau_{\text{tl}} \gtrsim 0.1$ and $y_{\text{tl}} \gtrsim 0.3$ for parameters yielding $\epsilon_q > 0.2$, while $\tau_{\text{tl}} < 0.01$ and $y_{\text{tl}} < 0.05$ for $\epsilon_q < 0.05$.

A few solutions corresponding to different Θ_{top} are shown on the left panel of Figure 5. The solutions belonging to the same family may have y_{tl} differing by a few percent depending on the relative importance of Comptonization and bremsstrahlung in the loss of transported energy (see Appendix A). Each of these solutions has slightly different pressure at the base of the transition layer, which corresponds to a dimensionless ionization parameter

$$\Xi = \frac{F_h}{cP_{\text{gas}}}. \quad (47)$$

The actual solution of the corona structure is determined by the disk solution, in particular by the resulting value of the ionization parameter at the top of the disk. The value of the ionization parameter at the base of transition layer is relatively sensitive to the value of Θ_{top} , as e.g. a relative change of the top temperature, $\Delta\Theta/\Theta \sim 10^{-4}$, results in a change of ionization parameter, $\Delta\Xi/\Xi \sim 10^{-2}$, while the transported power varies then by only $\Delta\epsilon_q/\epsilon_q \sim 10^{-4}$.

As discussed in section 2.4, the value of ϕ_s is not exactly determined. Therefore, we checked the sensitivity of the results to the value of ϕ_s (see Figure 6). It appears that the level of that sensitivity is determined by the optical depth of the corona. For higher optical depths ($\tau \sim 0.3$), the solution depends very weakly on the exact value of ϕ_s . However, for low optical depth ($\tau < 0.1$), ϵ_q increases significantly with increasing ϕ_s for $\phi_s < 0.6$, but levels off at higher ϕ_s .

5. DISCUSSION AND SUMMARY

We have developed a model of thermal conduction in a hot, active region situated above the surface of much colder matter. The model is applicable to regions with approximately plane parallel geometry so that the heat conduction equation may be reduced to one dimension. It applies also to localized active regions with, e.g., pillbox geometry (Stern et al. 1995), except for eq. (8) in which the deficit of soft photons must be taken into account.

The importance of thermal conduction in accretion disk coronae depends strongly on the local compactness parameter. For *ep* plasma the conduction has a negligible effect for $\ell_{\text{diss,loc}} > 0.1$ independent of other parameters. Pairs increase the importance of conduction by raising the sound speed, and therefore the maximum (saturated) heat flux. Our approach to pair coronae is highly simplified (a pure e^\pm corona and an e^\pm transition layer, no energy losses in a coronal wind) and is aimed to estimate the maximum effect of thermal conduction. Even in this highly idealized situation, conduction is important only for $\ell_{\text{diss,loc}} < 1$.

The value of $\ell_{\text{diss,loc}}$, crucial for the conduction problem, depends on the luminosity and geometrical parameters of the active region. E.g., for an electron-proton corona extending over the total surface of the accretion disk ($A \simeq \pi R^2$) we find from the definition of the local compactness, using eq. (35) and $r \sim 20$,

$$\ell_{\text{diss,loc}} = 54 \Theta_c^{1/2} \frac{L}{L_{\text{Edd}}}. \quad (48)$$

Then for $10^{-3} < L/L_{\text{Edd}} < 1$ and $0.2 < \Theta < 1$ we can expect local compactnesses ranging from 0.02 to 54. In this case conduction is important for $L \lesssim 10^{-2} L_{\text{Edd}}$, a condition which may apply in at least some AGN. On the other hand, a luminosity of $\sim 10^{-2} L_{\text{Edd}}$ is typical, e.g., for the hard state of the Galactic black hole candidate Cyg X-1 (e.g., Philips et al. 1996). Thus, conduction is likely to be important in at least some AGNs and Galactic black hole candidates.

When conduction becomes important, a nonuniform temperature distribution is established in the corona. In addition, a relatively hot transition layer between the corona and the disk is formed. In this case, the coronal radiation has a spectrum steeper than in models without conduction (with the same τ_{tot} and $\ell_{\text{diss,loc}}$). Moreover, the spectrum will have a more complicated form than a simple power-law. In particular, we expect a soft power-law-like emission from the transition layer due to Comptonization of soft photons from the disk in addition to the coronal emission. The spectral index of this emission should be larger than the spectral index of the coronal emission, as the Compton parameter of the transition layer is lower than the Compton parameter of the corona, except for very low local compactness $\ell_{\text{diss,loc}} \lesssim 0.01$. The superposition of the transition layer component on the spectrum of the coronal radiation (the latter extends to higher energies due to higher temperature in the corona) is a possible explanation of the formation of soft X-ray excesses, observed in many AGNs at energies below ~ 1 keV (e.g., Wilkes & Elvis 1987; Turner & Pounds 1989). When conduction is not important, the corona is isothermal and a rather sharp transition occurs at the corona base to the region in radiative equilibrium.

This research has been supported by Polish KBN grants 2P03D01008 and 2P03D01111 and NASA grant NAGW-3156.

A. Θ_{top}

We discuss here the criteria for adjusting Θ_{top} .

Θ_{top} determines the fraction of energy released in the corona that must be transported out of corona by conduction. For a lower Θ_{top} , Comptonization is less efficient and a higher flux must be carried down at lower plasma conductivity ($\propto \Theta^{5/2}$), which requires higher temperature gradient. Thus the decrease of Θ_{top} implies both the increase of the heat flux at the corona bottom, q_0 , and the decrease of the temperature at the corona bottom, Θ_0 . The total energy transported by conductive flux is radiated away in the transition layer. At the base of the transition layer the solution should have a vanishing conductive flux (as no flux can be transported further down due to very small plasma conductivity) and small temperature (determined by radiative equilibrium). Below we present analytic solutions for the transition layer structure in certain approximations to show qualitative properties of the solution, which constrain the possible value of Θ_{top} .

We consider the classical heat flux limit approximation with constant pressure, $P_{\text{gas}} = \text{const}$, and we neglect Compton heating. Below we use the dimensionless heat flux and pressure,

$$\tilde{q} \equiv -q_{\text{class}} h \frac{\sigma_T}{m_e c^3} = a \Theta^{5/2} \Theta', \quad (\text{A1})$$

$$\tilde{P} \equiv P_{\text{gas}} h \frac{\sigma_T}{m_e c^2} = 2 \Theta \tau_x. \quad (\text{A2})$$

For most of the transition layer, the temperature is sufficiently high (and the electron density sufficiently low) for cooling to be completely dominated by Comptonization. We consider then the heat transfer equation with the cooling term determined by Compton cooling,

$$\frac{d\tilde{q}}{dx} = 4 \Theta \tau_x \ell_{\text{diss,loc}} (\ell_s + \ell_h) / \ell_{\text{diss}}. \quad (\text{A3})$$

Eqs. (A1) and (A3), with the boundary conditions determined by the solution at the corona bottom, \tilde{q}_0 and Θ_0 , have the following solution

$$\Theta = \left(\frac{7\ell\tilde{P}}{2a} x^2 + \frac{7\tilde{q}_0}{2a} x + \Theta_0^{7/2} \right)^{2/7}, \quad \tilde{q} = 2\ell\tilde{P}x + \tilde{q}_0, \quad (\text{A4})$$

where $\ell \equiv \ell_{\text{diss,loc}} (\ell_s + \ell_h) / \ell_{\text{diss}}$. We see that for a given value of \tilde{q}_0 there is a unique value of $\Theta_0^{\text{max}} = [7\tilde{q}_0^2 / (8a\ell\tilde{P})]^{2/7}$ for which vanishing of \tilde{q} at the bottom of the transition layer is accompanied by Θ decreasing to a very small value. For higher Θ_0 temperature does not decrease and if we tried to prolong the solution further down the temperature would increase implying a negative temperature gradient. The physical meaning of that class of solutions [with $\Theta_0 > \Theta_0^{\text{max}}(\tilde{q}_0)$] is that conductive transport from the disk is required, in addition to \tilde{q}_0 , in order to provide sufficient amount of energy to the transition layer to balance the Compton cooling rate determined by Θ_0 . On the other hand, for $\Theta_0 < \Theta_0^{\text{max}}$ the temperature vanishes before the transported thermal energy can be radiated away due to Comptonization (in this case, the decrease of Θ to zero is accompanied with divergence of Θ' fast enough to keep the heat flux at a finite value). The decrease of Θ implies, however, the increase of τ_x and thus bremsstrahlung becomes efficient as a cooling mechanism. To check whether bremsstrahlung may provide sufficiently high cooling rate for

the loss of the rest of the transported thermal energy we consider the heat conduction equation with the cooling term determined by bremsstrahlung. We use the bremsstrahlung cooling rate for the nonrelativistic case and neglect the second term in parentheses in eq. (18), namely $1.781\Theta^{1.84}$, for calculational simplicity. Then,

$$\frac{d\tilde{q}}{dx} = \ell_b \tau_x^2 \Theta^{1/2}, \quad (\text{A5})$$

where $\ell_b = 4\sqrt{2}\alpha_f\pi^{-3/2}$. Eqs. (A1) and (A5) have the solution,

$$\tilde{q} = a \left[\frac{\ell_b \tilde{P}^2}{4a} (\Theta^2 - \Theta_b^2) + \left(\frac{\tilde{q}_b}{a} \right)^2 \right]^{1/2}, \quad (\text{A6})$$

where \tilde{q}_b and Θ_b are the heat flux and the temperature at the point where bremsstrahlung starts to dominate. For $\Theta_b < 2\tilde{q}_b/\sqrt{\ell_b \tilde{P}^2 a}$, the energy transported by the conductive flux cannot be radiated away. This means that certain Θ_0^{\min} exists such that for lower Θ_0 no acceptable solution exists, because \tilde{q}_b and Θ_b are positively correlated with \tilde{q}_0 and Θ_0 , respectively.

The solution of eqs. (38–40) has the same qualitative properties as the approximation we investigated above. A certain range of the values of Θ_0 exists then, $(\Theta_0^{\min}, \Theta_0^{\max})$, for which we obtain physically acceptable solutions. For lower Θ_0 , the energy that enters the transition layer cannot be radiated away and as a result the temperature in the layer would increase leading to the increase of Θ_0 . On the other hand, for higher Θ_0 the energy delivered to the layer is too low to maintain its temperature and the temperature would decrease. Solutions corresponding to different $\Theta_0^{\min} < \Theta_0 < \Theta_0^{\max}$ differ with respect to the relative importance of bremsstrahlung and Compton cooling in the loss of transported energy.

As discussed above, the decrease of Θ_{top} implies a decrease of Θ_0 and an increase of \tilde{q}_0 . As the value of \tilde{q}_0 is constrained by the saturation effect (see section 4), the above constraints on Θ_0 imply the existence of a certain range of the values of Θ_{top} for which the correct behaviour of the solution in the transition layer can be obtained. In our calculation procedure (section 2.7), we determine this range by looking at the behaviour of the solution at the bottom end for different values of Θ_{top} .

REFERENCES

- Balbus, S. A. & McKee, C. F. 1982, *ApJ*, 252, 529
- Björnsson, G. & Svensson, R. 1992, *ApJ*, 394, 500
- Cowie, L. L. & McKee, C. F. 1977, *ApJ*, 211, 135
- Done C., & Fabian A. C. 1989, *MNRAS*, 240, 81
- Ghisellini, G., Haardt, F. & Fabian A. C. 1993, *MNRAS*, 263, L9
- Gierliński, M., Zdziarski, A. A., Done C., Johnson, W. N., Ebisawa, K., Ueda, Y., Haardt, F. & Philips, B. F. 1997, *MNRAS*, in press
- Giuliani, J. L. 1984, *ApJ*, 277, 605
- Gondek, D., Zdziarski, A. A., Johnson, W. N., George, I. M., McNaron-Brown, K., Magdziarz, P., Smith, D. & Gruber, D. E. 1996, *MNRAS*, 282, 646
- Haardt, F. & Maraschi, L. 1991, *ApJ*, 380, L51
- Haardt, F. & Maraschi, L. 1993, *ApJ*, 413, 507

- Phlips, B. F., et al. 1996, *ApJ*, 465, 907
- Pietrini, P. & Krolik, J. H. 1995, *ApJ*, 447, 526
- Poutanen, J. & Svensson, R. 1996, *ApJ*, 470, 249
- Róžańska, A. & Czerny, B. 1996, *Acta Astronomica*, 46, 233
- Shimura, T., Mineshige S. & Takahara, F. 1995, *ApJ*, 439, 74
- Sincell, M. & Krolik, J. H. 1997, *ApJ*, in press
- Spitzer, L. 1962, *Physics of Fully Ionized Gases* (New York: Interscience Publishers)
- Stern, B. E., Poutanen, J., Svensson, R., Sikora, M. & Begelman, M. C., 1995, *ApJ*, 449, L13
- Svensson, R. 1982, *ApJ*, 258, 335
- Svensson, R. 1996, *A&AS*, 120, 475
- Svensson, R. & Zdziarski, A. A. 1994, *ApJ*, 436, 599
- Turner, P. J. & Pounds, K. A. 1989, *MNRAS*, 240, 833
- Wilkes, B. J. & Elvis, M. 1987, *ApJ*, 323, 243
- Zdziarski, A. A., Fabian, A. C., Nandra, K., Celotti, A., Rees, M. J., Done, C., Coppi, P. S. & Madejski, G. M. 1994, *MNRAS*, 269, L55
- Zdziarski, A. A., Johnson, W. N., Done, C., Smith, D. & McNaron-Brown, K. 1995, *ApJ*, 438, L63
- Zdziarski, A. A., Johnson, W. N., Poutanen, J., Magdziarz, P. & Gierliński, M. 1997, *Proceedings of the 2nd INTEGRAL Workshop*, in press

Fig. 1.— The dependence of ϵ_q on $\ell_{\text{diss,loc}}$ in electron-positron plasmas for the value of $\phi_s = 0.3$ (solid curves) compared to the classical heat flux approximation (dotted curve). For solid curves $\tau_{\text{tot}} = 0.06, 0.1$ and 0.2 from top to bottom and for the dotted curve $\tau_{\text{tot}} = 0.1$. For $\ell_{\text{diss,loc}} > 1$, $\epsilon_q \propto \ell_{\text{diss,loc}}^{-1}$ for the solid curves.

Fig. 2.— The same as in Figure 1 but for electron-proton plasmas with $\tau_{\text{tot}} = 0.1$; $\epsilon_q \propto \ell_{\text{diss,loc}}^{-1}$ for $\ell_{\text{diss,loc}} > 0.04$.

Fig. 3.— ϵ_q as a function of the optical depth of the corona.

Fig. 4.— The corona and transition layer structure obtained in our model (solid curves) and the solution of the model neglecting conduction (dotted curves) for electron-proton coronae with $\ell_{\text{diss,loc}} = 0.01$ (left panel) and 0.03 (right panel) and $\tau_{\text{tot}} = 0.1$. The curves show (a) the temperature, (b) the electron density in the units of $\tau_x = n_e(x)\sigma_T h$, and (c) the heat flux absolute value $|q|$ with respect to the power dissipated per surface area, L_{diss}/A . For $\ell_{\text{diss,loc}} = 0.01$ solution is obtained for $\Theta_{\text{top}} = 0.52466$. The solution gives $\epsilon_q = 0.5$, the ionization parameter at the base of the transition layer, $\Xi = 0.004$, and the optical depth and Compton parameter in the transition layer, $\tau_{\text{tl}} = 0.4$ and $y_{\text{tl}} = 0.6$, respectively. The absolute range of possible Θ_{top} is $\Delta\Theta = 1.5 \times 10^{-5}$, which yields $\Delta\epsilon_q = 2 \times 10^{-5}$ and $\Delta\Xi = 1.5 \times 10^{-4}$. For $\ell_{\text{loc}} = 0.03$, the solution, with $\Theta_{\text{top}} = 0.618353$, gives $\epsilon_q = 0.2$, $\Xi = 0.04$, $\tau_{\text{tl}} = 0.2$, $y_{\text{tl}} = 0.3$, $\Delta\Theta = 1 \times 10^{-6}$, $\Delta\epsilon_q = 3 \times 10^{-6}$, $\Delta\Xi = 10^{-3}$. The break of $|q|A/L_{\text{diss}}$ at the interface between the transition layer and the corona ($x = 0$) is due to the fact that the corona is efficiently heated by dissipation, whereas only the much smaller Compton heating takes place in the transition layer.

Fig. 5.— The same as in Figure 4 but for electron-positron plasmas, $\ell_{\text{diss,loc}} = 0.1$ (left panel) and 1 (right panel) and $\tau = 0.1$. For $\ell_{\text{diss,loc}} = 0.1$, the solution gives $\Theta_{\text{top}} = 0.63155$, $\epsilon_q = 0.2$, $\Xi = 0.3$, $\tau_{\text{tl}} = 0.12$ and $y_{\text{tl}} = 0.3$, $\Delta\Theta = 5 \times 10^{-5}$, $\Delta\epsilon_q = 3 \times 10^{-4}$, $\Delta\Xi = 10^{-2}$. For $\ell_{\text{diss,loc}} = 1$, we get $\Theta_{\text{top}} = 0.650531$, $\epsilon_q = 0.05$, $\Xi = 3.6$, $\tau_{\text{tl}} = 0.02$ and $y_{\text{tl}} = 0.05$, $\Delta\Theta = 10^{-6}$, $\Delta\epsilon_q = 3 \times 10^{-4}$, $\Delta\Xi = 1.5 \times 10^{-2}$. The three solid curves on the left panel show solutions corresponding to three different values of Θ_{top} .

Fig. 6.— The dependence of ϵ_q on ϕ_s . Left panel: electron-positron plasmas, $\ell_{\text{diss,loc}} = 0.12, 0.12, 1.2, 1.2$ and $\tau_{\text{tot}} = 0.06, 0.3, 0.06, 0.3$ from top to bottom. Right-panel: electron-proton plasmas, $\ell_{\text{diss,loc}} = 0.01, 0.01, 0.08, 0.08$ and $\tau_{\text{tot}} = 0.1, 0.32, 0.1, 0.32$ from top to bottom.

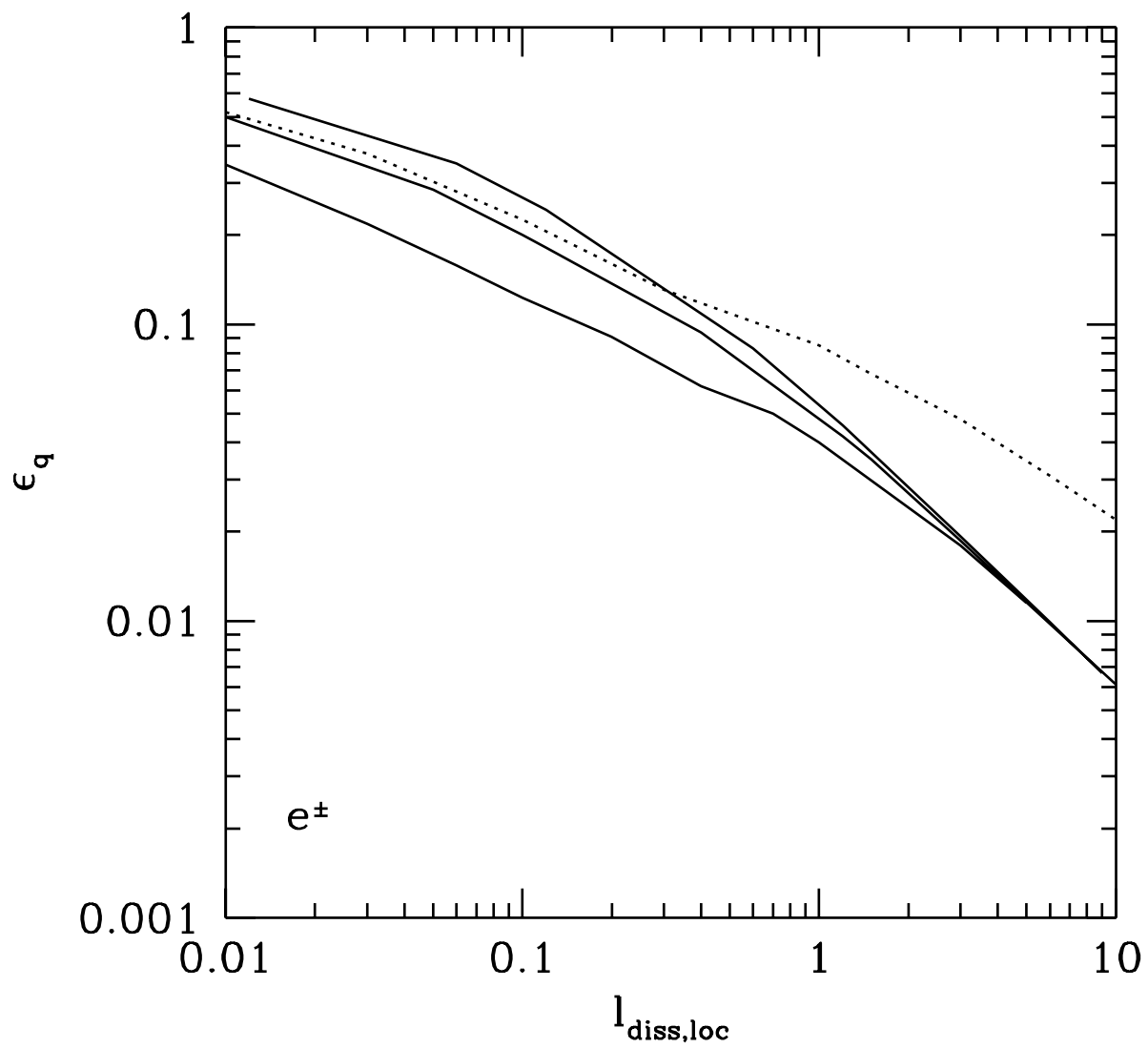


Fig. 1

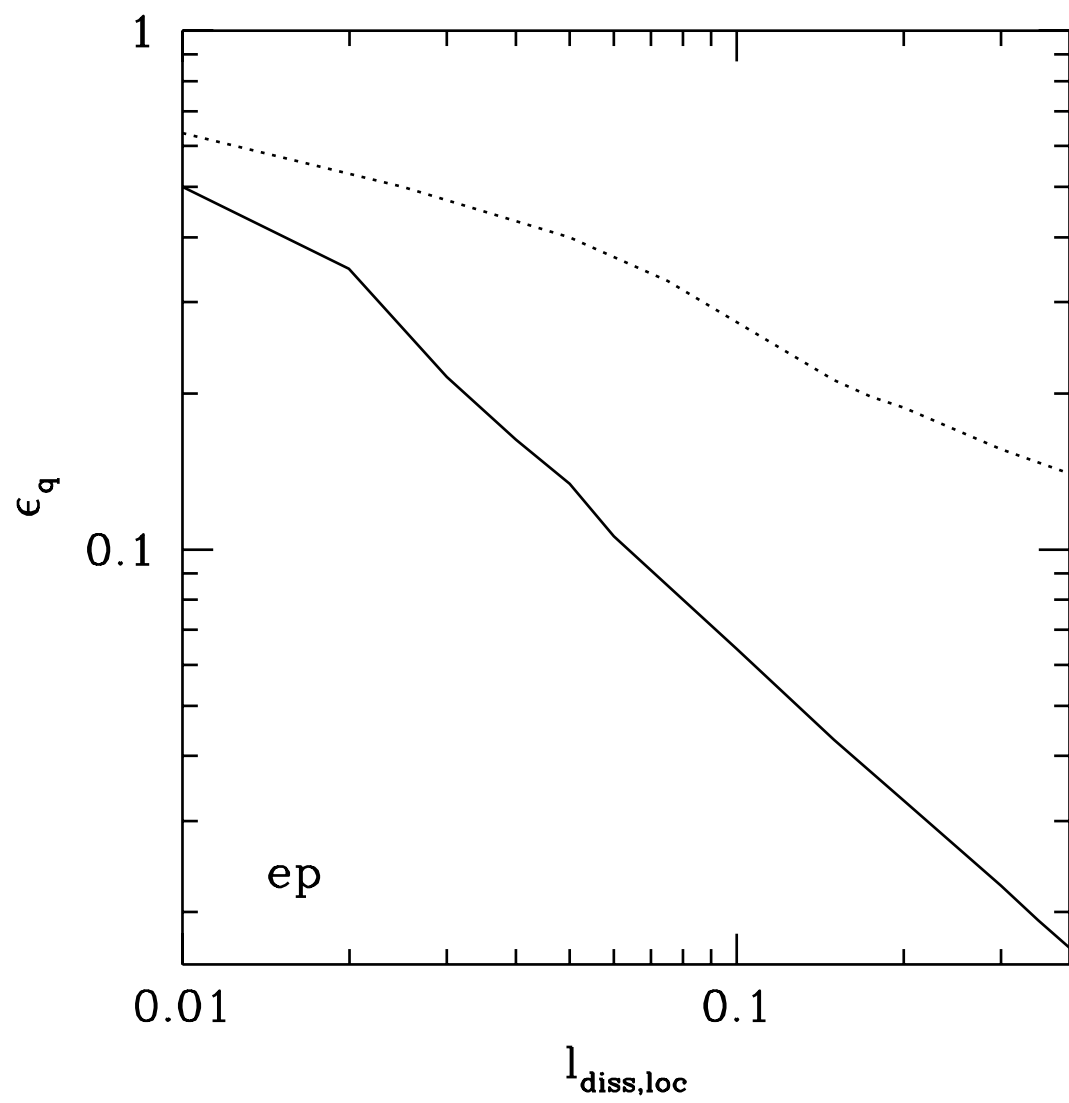


Fig. 2

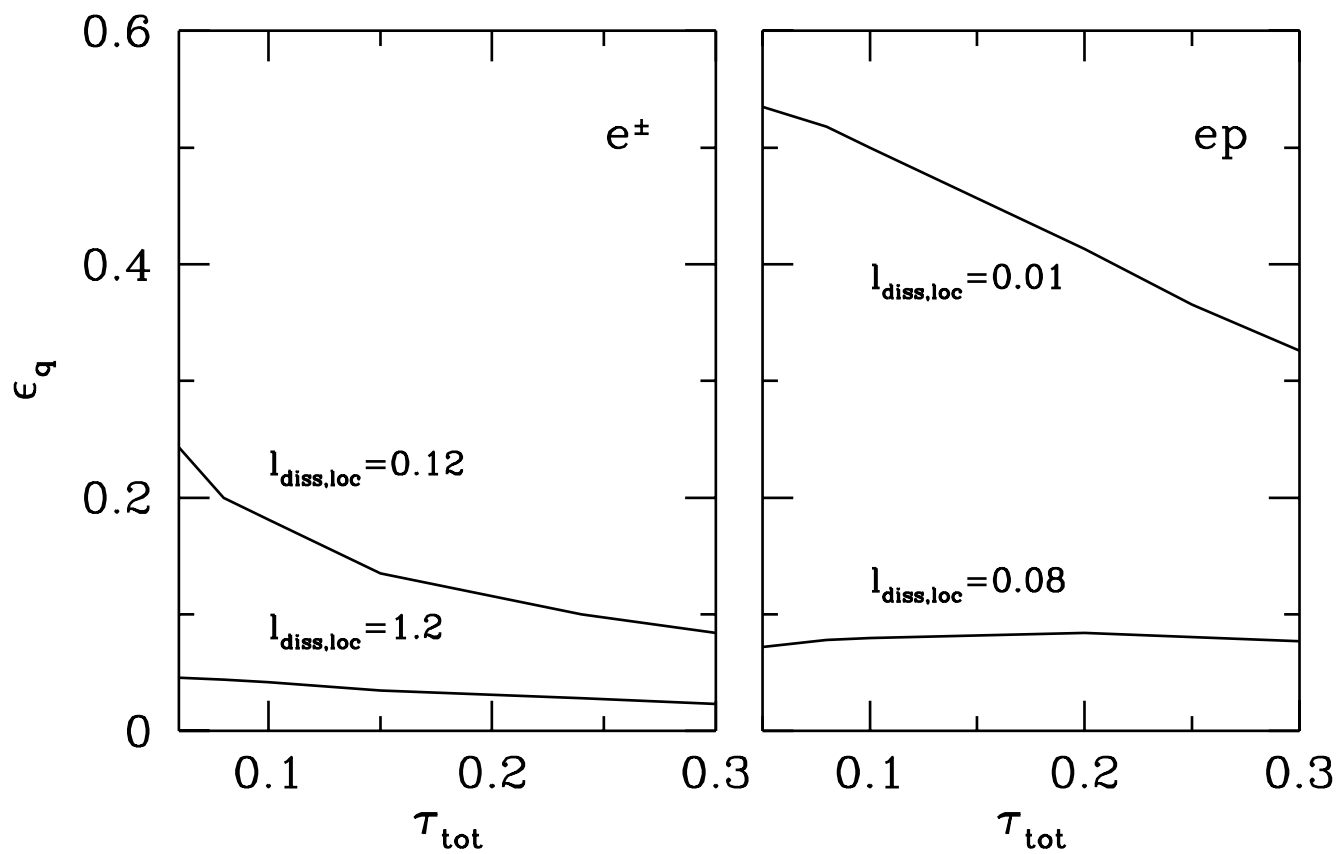


Fig. 3

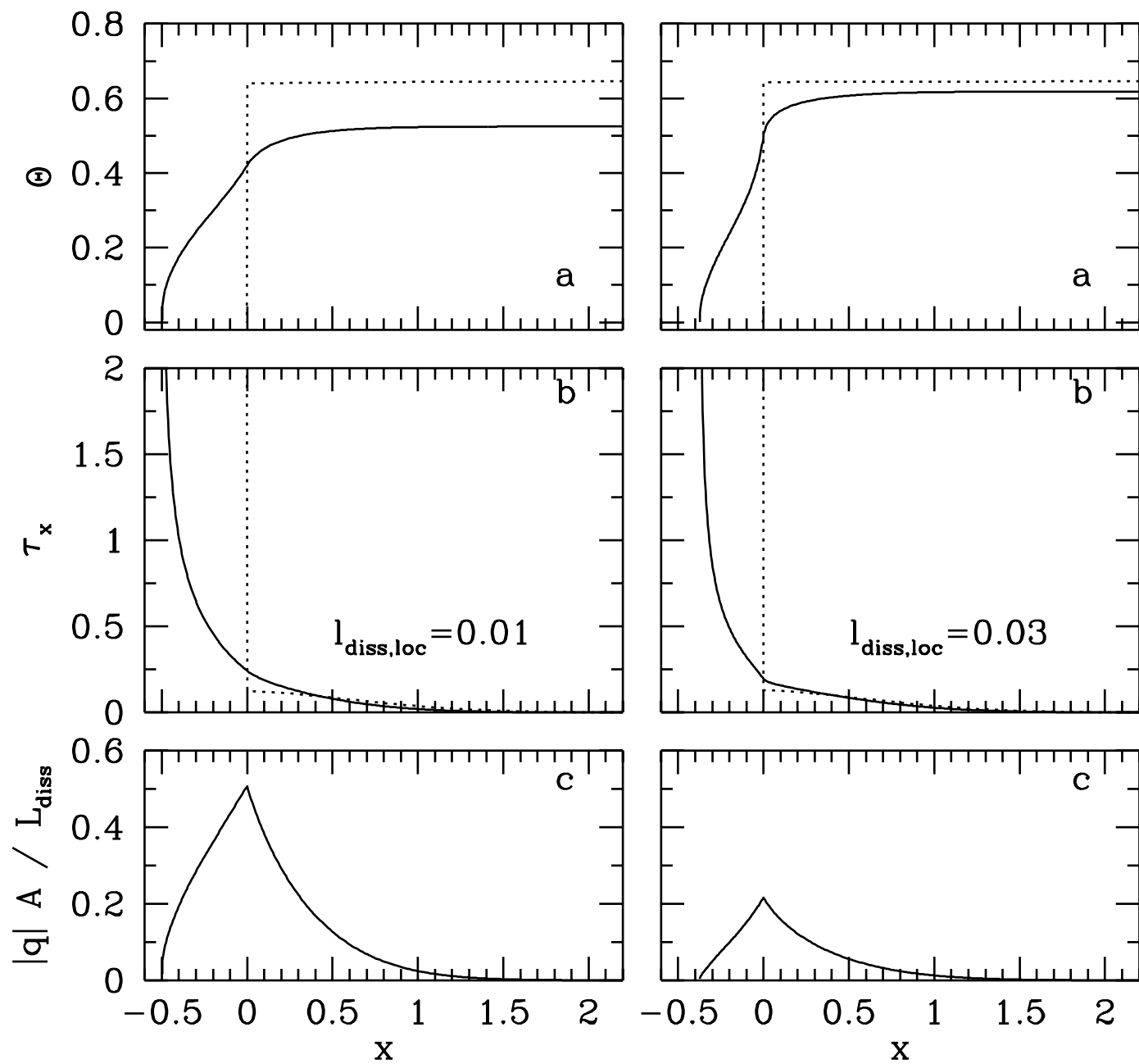


Fig. 4

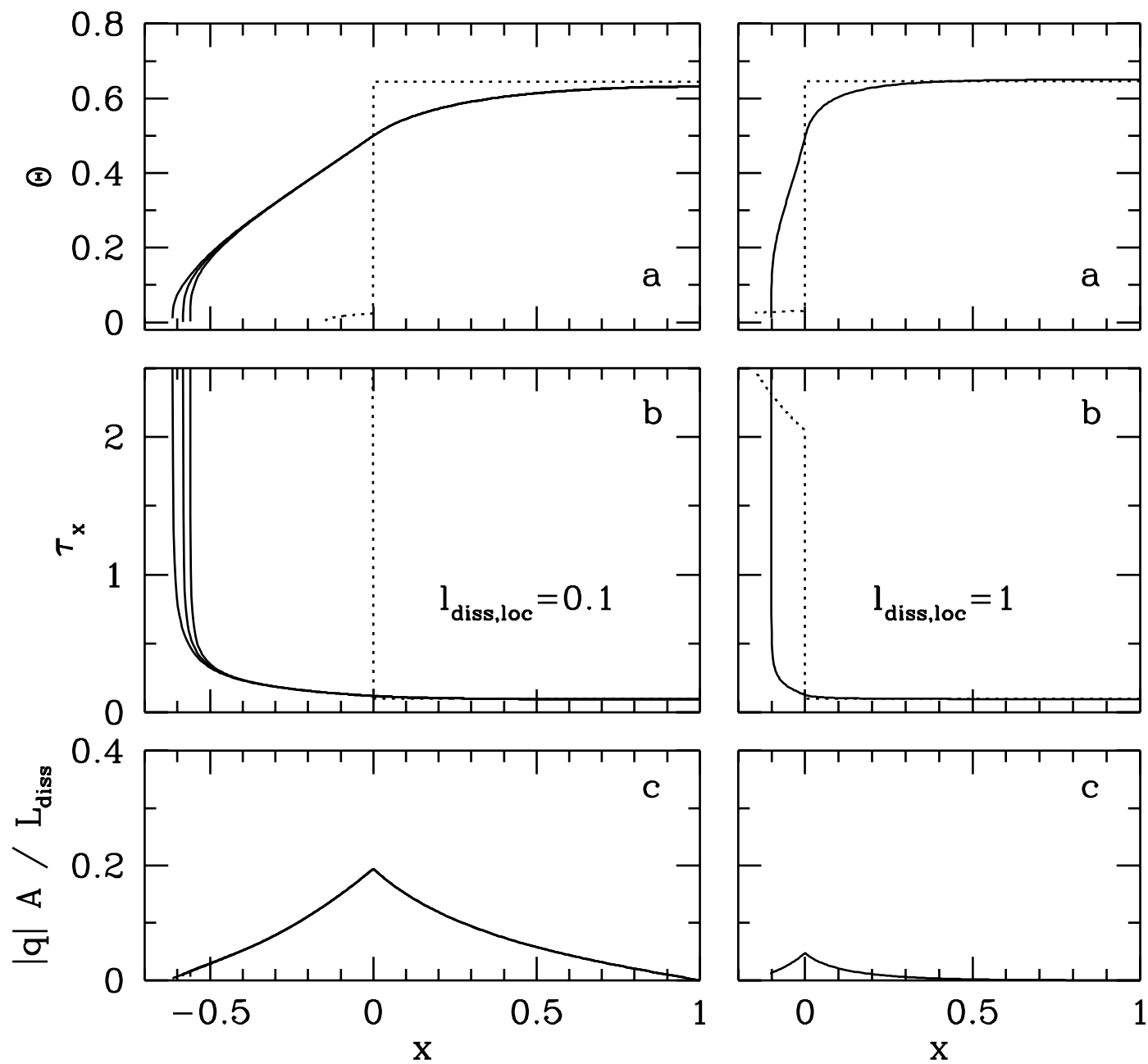


Fig. 5

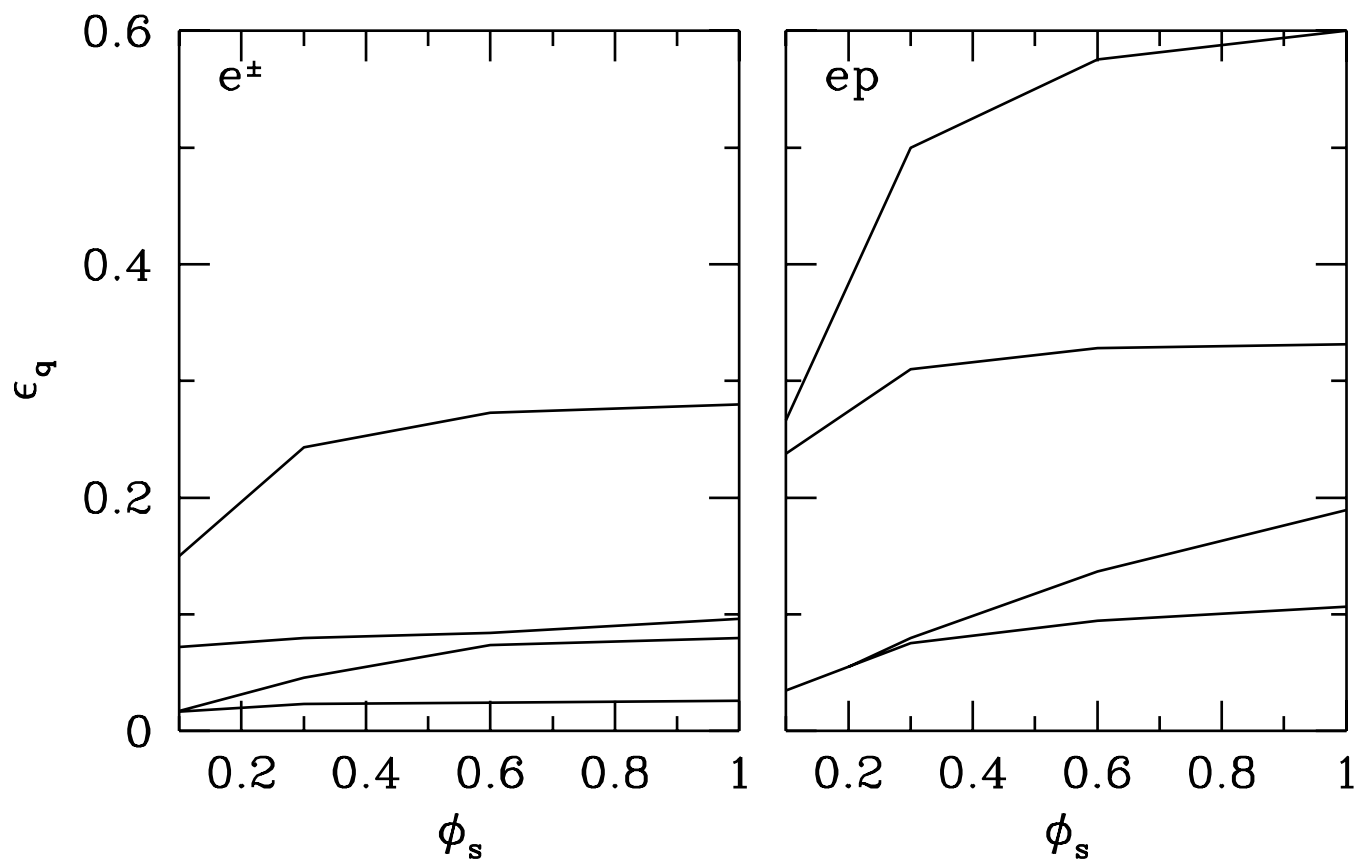


Fig. 6